



KTH Electrical Engineering

High Power Microwave Sources: Design and Experiments

CECILIA MÖLLER

Licentiate Thesis
Stockholm, Sweden 2011

TRITA-EE 2011:046
ISSN 1653-5146
ISBN 978-91-7501-044-1

KTH Rymd- och plasmafysik
Skolan för elektro- och systemteknik
100 44 Stockholm

Akademisk avhandling som med tillstånd av Kungl Tekniska högskolan framlägges till offentlig granskning för avläggande av teknologie licentiat-examen i fysikalisk elektroteknik fredagen den 10 juni 2011 klockan 10.15 i Seminarierummet, Avdelningen för rymd- och plasmafysik, Teknikringen 31, Kungl Tekniska högskolan, Stockholm.

© Cecilia Möller, juni 2011

Tryck: Universitetsservice US AB

Abstract

High-Power Microwaves (HPM) can be used to intentionally disturb or destroy electronic equipment at a distance by inducing high voltages and currents.

This thesis presents results from experiments with a narrow band HPM source, the vircator. The high voltages needed to generate HPM puts the vircator under great stress, especially the electrode materials. Several electrode materials have been tested for endurance and their influence on the characteristics of the microwave pulse. With the proper materials the shot-to-shot variations are small and the geometry can be optimized in terms of e.g. output power or frequency content. Experiments with a resonant cavity added to the vircator geometry showed that with proper tuning of the cavity, the frequency content of the microwave radiation is very narrow banded and the highest radiated fields are registred.

Since HPM pulses are very short and have high field strengths, special field probes are needed. An HPM pulse may shift in frequency during the pulse so it is very important to be able to compensate for the frequency dependence of the entire measurement system. The development and use of a far-field measurement system is described.

Sammanfattning

Mikrovågor med hög effekt, HPM (från engelskans High Power Microwaves), kan användas till att medvetet störa eller förstöra elektronik genom att inducera höga strömmar och spänningar.

Denna avhandling redovisar resultat från experiment med en virkator, en smalbandig HPM-källa. För att generera en HPM-puls krävs en mycket hög spänning. Detta belastar virkatorn hårt och det är framför allt elektrodmaterialen som riskerar att förstöras. Flera elektrodmaterial har testats för att undersöka deras hållbarhet och inflytande på mikrovågspulsen. Med rätt material blir skillnaderna mellan två identiska försök små och man kan utföra optimeringsstudier av geometrin, t ex med avseende på utstrålad effekt eller frekvensinnehåll i mikrovågspulsen. Experiment har visat att virkatrons utstälade effekt kan ökas genom att inkludera en resonanskavitet i geometrin. När kaviteten är rätt inställd blir virkatorn mycket smalbandig.

Eftersom en HPM-puls har mycket hög effekt och pulslängden är kort behövs speciella fältprober. Frekvensen kan dessutom variera under pulsen så det är mycket viktigt att kompensera för mätsystemets frekvensberoende. Utvecklingen av frifältsprober för HPM är också beskriven i denna avhandling.

Preface

I have worked at the Swedish Defence Research Agency (FOI) since 2003 with development of HPM weapon sources and measurement technique. The HPM weapon research is located at Grindsjön, a test site 40 km south of Stockholm. In the mid 1980's HPM protection research started in Linköping and in the 1990's weapon research started in Grindsjön. In the beginning the weapon research was focused on small explosively driven voltage generators. In the early 2000's the research focus shifted to compact HPM sources that can be used repetitively, pulsed power supply and HPM measurement technique. Since 2006 I have performed part time PhD studies at KTH on HPM sources and HPM measurement technique.

Acknowledgements

First of all I would like to thank my colleague and friend Mattias Elfsberg, with whom I have made the experiments and analysis.

I would also like to thank my supervisors, Nils Brenning at KTH, Anders Larsson and Tomas Hurtig at FOI and the manager of the HPM project at FOI, Sten E. Nyholm.

List of Papers

This thesis is based on the work presented in the following papers. At FOI the authors, except the main author, are listed alphabetically. I changed my last name from Nylander to Möller in 2006.

- I M. Elfsberg, T. Hurtig, A. Larsson, **C. Möller** and S. Nyholm, "Experimental Studies of Anode and Cathode Materials in a Repetitive Driven Axial Vircator", *IEEE Trans. Plasma Sci.*, vol. 36, pp. 688–693, 2008.

This paper was originally presented in a shorter version, conference paper XVI, at the IEEE Pulsed Power and Plasma Science Conference in Albuquerque 2007. I have planned and performed the experiments and made the analysis of the microwave radiation data, but I was on maternity leave when the paper was written.

- II **C. Möller**, M. Elfsberg, A. Larsson and S. Nyholm, "Magnetic Field Measurement System for HPM Research", in *Proc. of Radiovetenskap och kommunikation (RVK 2008)*, pp. 250–253, Växjö, Sweden, 9–11 June 2008.

I have developed the post processing method for the microwave measurements and designed and built the baluns.

- III **C. Möller**, M. Elfsberg, A. Larsson and S. Nyholm, "Experimental Studies of the Influence of a Resonance Cavity in an Axial Vircator", *IEEE Trans. Plasma Sci.*, vol. 38, pp. 1318–1324, 2010.

This paper is a longer version of the conference paper XIX that I presented at the IEEE Pulsed Power Conference in Washington 2009. I have planned and performed the experiments, made the analysis of the microwave radiation data and made PIC simulations.

Journal papers not included in the thesis

- IV B. Novac, M. Istenič, J. Luo, I. Smith, J. Brown, M. Hubbard, P. Appelgren, M. Elfsberg, T. Hurtig, C. Möller, A. Larsson and S. Nyholm, "A 10-GW Pulsed Power Supply for HPM Sources", *IEEE Trans. Plasma Sci.*, vol. 34, pp. 1814–1821, 2006.
- V P. Appelgren, M. Akyuz, M. Elfsberg, T. Hurtig, A. Larsson, S. Nyholm and C. Möller, "Study of a Compact HPM System With a Reflex Triode and a Marx Generator", *IEEE Trans. Plasma Sci.*, vol. 34, pp. 1796–1805, 2006.
- VI C. Möller, T. Hurtig, A. Larsson and S. Nyholm, "Numerical Simulation of the TE11 Mode in a Coaxial Vircator", *IEEE Trans. Fundamentals and Materials* (Japan), vol. 127, pp. 687–692, 2007.
- VII S. Nyholm, M. Akyuz, P. Appelgren, M. Elfsberg, T. Hurtig, A. Larsson, C. Möller, "Studies of vircator operation at FOI: Electrode material erosion studies", *Journal of Directed Energy*, vol. 3, pp. 39–53, 2008.
- VIII C. Möller, M. Elfsberg, T. Hurtig, A. Larsson and S. Nyholm, "Proof of principle experiments on direct generation of the TE11 mode in a Coaxial Vircator", *IEEE Trans. Plasma Sci.*, vol. 8, pp. 26–31, 2010.

Conference papers not included in the thesis

- IX B. Novac, M. Istenič, J. Luo, I. Smith, J. Brown, M. Hubbard, P. Appelgren, M. Elfsberg, T. Hurtig, C. Nylander, A. Larsson and S. Nyholm, "A 10 GW Pulsed Power Supply for HPM Sources", in "Proc. of 15th IEEE International Pulsed Power Conference (PPC), Monterey, California, USA", 13–17 July 2005.
- X M. Karlsson, F. Olsson, G. Filipsson, E. Edbom, B.-O. Bergman, T. Hurtig, P. Appelgren, M. Elfsberg, A. Larsson, C. Nylander and S. Nyholm, "Comparison Between Experimental And Numerical Studies Of A Reflex Triode", in "Proc. of 15th IEEE International Pulsed Power Conference (PPC), Monterey, California, USA", 13–17 July 2005.

- XI T. Hurtig, C. Nylander, P. Appelgren, M. Elfsberg, A. Larsson and S. Nyholm, "Initial Results From Experiments With A Reflex Triode Powered By A Marx Generator", in "Proc. of 15th IEEE International Pulsed Power Conference (PPC), Monterey, California, USA", 13–17 July 2005.
- XII C. Möller, T. Hurtig, A. Larsson and S. Nyholm, "Electron Beam Deviation due to Lorentz Force in Reflex Triode", in "Proc. of 1st Euro-Asian Pulsed Power Conference (EAPPC), Chengdu, Sichuan, China", 18–22 September 2006.
- XIII T. Hurtig, C. Möller, A. Larsson and S. Nyholm, "Numerical Simulation of Direct Excitation of the TE₁₁ Mode in a Coaxial Vircator", in "Proc. of 1st Euro-Asian Pulsed Power Conference (EAPPC), Chengdu, Sichuan, China", 18–22 September 2006.
- XIV S. Nyholm, M. Akyuz, P. Appelgren, T. Hurtig, A. Larsson and C. Nylander, "Experiments with and Simulations of a Reflex Triode Vircator", in "Proc. of American Electro-Magnetics Conference (AMEREM), Albuquerque, New Mexico, USA", 9–14 July 2006.
- XV S. Nyholm, M. Akyuz, P. Appelgren, M. Elfsberg, T. Hurtig, A. Larsson, C. Möller and M. Skoglund, "Studies of repetitive vircator operation", in "Proc. of 7th Int. All-Electric Combat Vehicle Conf., Stockholm, Sweden", 11–13 June 2007.
- XVI M. Elfsberg, T. Hurtig, A. Larsson, C. Möller and S. Nyholm, "Experimental studies of anode and cathode materials in a repetitive-driven axial vircator", in "Proc. of 2007 IEEE Pulsed Power and Plasma Science Conference, Albuquerque, USA", 7–22 June 2007.
- XVII S. Nyholm, M. Akyuz, P. Appelgren, M. Elfsberg, T. Hurtig, A. Larsson and C. Möller, "Studies of vircator operation at FOI - electrode material erosion studies", in "Proc. of Tenth Annual Directed Energy Symposium, Huntsville, USA", 5–8 November 2007.
- XVIII A. Larsson, M. Akyuz, P. Appelgren, M. Elfsberg, T. Hurtig, C. Möller and S. Nyholm, "Research on Narrow-Band High-Power Microwave Sources Performed at FOI", in "Proc. of Radiovetenskap och kommunikation (RVK 2008), Växjö, Sweden", 9–11 June 2008.

- XIX C. Möller, M. Elfsberg, A. Larsson and S. Nyholm, "Experimental studies of the influence of a resonance cavity in an axial vircator", in "Proc. of 17th IEEE International Pulsed Power Conference, Washington, USA", 28 June – 2 July 2009.
- XX C. Möller, T. Hurtig, A. Larsson and S. Nyholm, "Numerical simulations of the influence of a reflector in a coaxial vircator", in Proc. of 17th IEEE International Pulsed Power Conference, Washington, USA", 28 June – 2 July 2009.
- XXI M. Elfsberg, T. Hurtig, C. Möller and S. Nyholm, "Experimental studies on a coaxial vircator operating in TE₁₁ mode", in "EAPPC, Korea", October 2010.

Contents

Preface	v
Acknowledgements	vii
List of Papers	ix
Contents	xiii
List of Figures	xv
1 Introduction	1
1.1 Narrow band HPM sources	3
1.2 Vircators	6
2 Experiments and theoretical models	9
2.1 Vircator theory	9
2.2 Experimental setup	12
2.3 Design tools	17
3 Results	21
3.1 Paper I	21
3.2 Paper II	21
3.3 Paper III	22
4 Discussion	25
5 Conclusions	27
References	29

List of Figures

1.1	Different HPM pulses. The upper figures shows the time domain and the lower the frequency domain. a) Narrow band b)Intermediate case c) Wide band	2
1.2	Magnetron. The electrons circle around the anode. When they slow down at the cavity gaps and form spokes, kinetic energy is transformed to electromagnetic radiation.	4
1.3	MILO. The current generates an axial magnetic field that prevents the electrons from short-circuiting the anode-cathode gap.	5
1.4	Reltron. The electron beam is bunched in the first cavity. The bunched beam is then accelerated to relativistic speed, which freezes the bunching. This leads to less velocity spread of the electrons and the radiation becomes monochromatic.	6
1.5	Schematic vircator. Electrons are emitted from the cathode and accelerated towards and then through the transparent anode. A virtual cathode is formed when the space charge limit is reached.	7
1.6	Three common vircator types. a) Axial vircator b) Coaxial vircator c) Reflex triode	8
2.1	Particle in cell simulation of an axial vircator showing the relative momentum of the electrons on the center axis. A virtual cathode is beginning to form at a distance of about the anode-cathode distance. Before a new virtual cathode is formed electrons escape from the virtual cathode area.	11
2.2	Schematic figure of the HPM lab.	12
2.3	HPM lab. The microwave radiation is propagated through a 2 m long waveguide. a) Marx generator, vircator and vacuum pump. b) Waveguide aperture in the anechoic chamber.	13

2.4	Axial vircator with different extraction possibilities. The adjustable cavity wall is used to tune the cavity. a) Extraction from both sides of the anode. b) Extraction only from the anode-cathode side. Radiation generated by the virtual cathode is not extracted.	14
2.5	a) Marx generator with 25 stages. Here only the last stage is visible. The capacitive voltage divider probe can also be seen. b) Circuit drawing with four stages. The capacitors C are charged in parallel and when the first spark gap is triggered, the rest of the spark gaps close. The capacitors are then discharged in series and the voltage over the load Z_L is four times the input voltage.	15
2.6	B-dot probe.	16
2.7	2D PIC grid	17
2.8	1D Yee scheme. The electric field is calculated at integer time and space steps while the magnetic field is calculated at half integer steps. The index is n for the time stepping and i for the space stepping.	18

1. Introduction

The idea to use an electromagnetic pulse to destroy or disturb electronic equipment originated from the electrical black-outs caused by nuclear weapon testing [1]. In a nuclear explosion a high power electromagnetic pulse (EMP) is generated. If such a pulse can be generated without a nuclear explosion it can be used as a nonlethal weapon, that only causes damage to electronics. This is the idea behind High Power Microwaves (HPM) [2, 3]. It is intended to be used to intentionally disturb or destroy electronic equipment without damaging infrastructure or hurting people.

The expected outcome of an HPM attack can be either a hard kill, where the electrical components are physically damaged, or a soft kill, where the components are disabled with malfunction as a result. In a hard kill the HPM pulse induces currents high enough to melt the metal on a circuit board, or a voltage that will result in a flashover in sensitive electrical components. A soft kill upsets a digital circuit when the produced voltage from the HPM pulse is of the same order as the operating voltage a semiconductor component, e.g. a transistor. To make a PC crash with a required manual restart, an electric field of some kV/m is needed [4]. The small scale of electronic circuits make them vulnerable to small amounts of energy.

To protect a device from HPM it has to be wholly contained inside a metal structure, a Faraday cage, so that the HPM pulse cannot penetrate the object. Most electrical devices need an external power supply and the radiation can couple in through these cables, despite otherwise good electrical shielding. Many devices also have some kind of communication device, such as an antenna or network connection with a cable, through which an HPM pulse can couple in. The way HPM is coupled into an object is divided into two types, front door and back door coupling. Front door coupling is through intentional receptors for electromagnetic energy, e.g. antennas and sensors. Back door coupling is through incoming cables, holes in the

structure like access panels, doors and windows, and bad weldings or other imperfections.

In general, the power coupled into an object depends on the area sensitive to radiation, the coupling cross section. For front door coupling this is often the area of a slot or the aperture area of an antenna. If the frequency of the HPM pulse is within the bandwidth of the antenna much energy is coupled in but the effect falls off rapidly for other frequencies. For back door coupling it is more complicated and the cross section depends on both frequency and position. The optimal coupling frequency for an object is hardly ever known beforehand.

There are two main approaches to use HPM; one is to use a narrow band source where the radiated energy is concentrated in a small frequency band, and the other is to use a wide band source where the energy is radiated over a large frequency band, see Figure 1.1. With a wide band source the chances are good that some energy is coupled in at a frequency where the object is sensitive, but the energy is small and the effects are also small. If a narrow band source is tuned to a frequency at which the target is sensitive, the effects can be large, but it is difficult to know what frequency will give the best coupling. A narrow band source that is tunable in frequency can cover a larger frequency band with several HPM pulses with different frequencies.

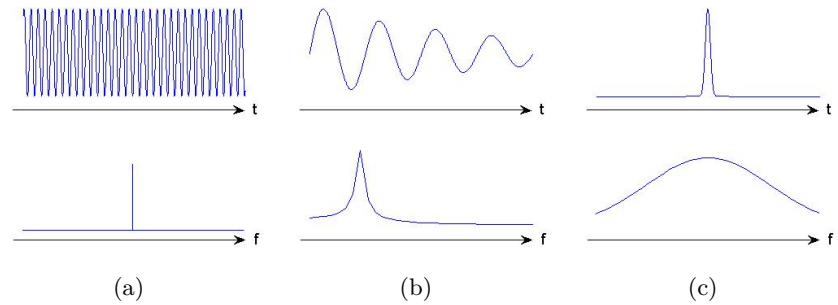


Figure 1.1: Different HPM pulses. The upper figures shows the time domain and the lower the frequency domain. a) Narrow band b) Intermediate case c) Wide band

For short pulses, less than 100 ns, thermal diffusion can be neglected and the power needed to damage a semiconductor component by a hard

kill varies as $1/t$. For longer pulses, between 100 ns and 1 μ s, energy is transported away by thermal diffusion and the power needed varies with $1/\sqrt{t}$. To damage an electrical component with a short pulse, little energy but high power is needed, whereas high energy and lower power is needed with a longer pulse.

One other way to enhance the effect of HPM is to use repetitive pulses. To obtain thermal stacking, where the energy has no time to diffuse between the pulses, a pulse repetition rate of more than 1 kHz is needed. It is however likely that much lower repetition rate will have effect since each pulse can degrade the material, with a lower threshold for damage than originally as a result.

The radiated power is depending on the physical size of the HPM system. Both the radiation source and the power supply get larger with power. Therefore the more powerful systems with radiated powers over 1 GW are best suited for stationary installations, e.g. on a war ship or on a site. When there are no limitations in space, large antennas can be used to focus the radiated beam.

Smaller systems with an output power of less than 1 GW can be mounted on vehicles, like a truck, or be used as HPM warheads in missiles.

In this thesis results from experiments with a narrow band source, a vircator, will be reported, as well as the development of a measurement system for HPM pulses.

1.1 Narrow band HPM sources

To generate powers over 100 MW vacuum based electronics are used. Microwave radiation is generated by converting the kinetic energy in an electron beam [2, 5]. The source is driven by a voltage pulse with an amplitude of about 100 kV-1 MV and a pulse length of about 1 μ s. The operating frequency is some GHz and quite narrow banded, due to the nature of the source. Some common narrow band HPM sources are the magnetron, the MILO, the reltron, and the vircator. In the magnetron a voltage is applied between the inner cathode and the outer anode, see Figure 1.2. Electrons are emitted from the cylindrical cathode, and due to the radial electric field and an external axial magnetic field, the electrons circle around the cathode. The radiation is often extracted from one vane in the anode. At the gaps

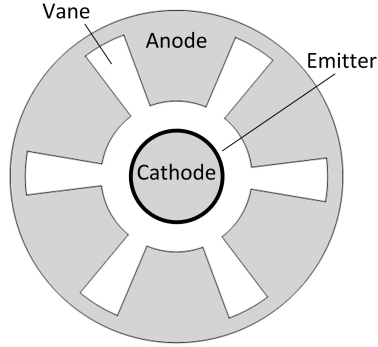


Figure 1.2: Magnetron. The electrons circle around the anode. When they slow down at the cavity gaps and form spokes, kinetic energy is transformed to electromagnetic radiation.

of the cavities the electrons slow down and electron spokes are formed. The kinetic energy of the electron beam is transformed to electromagnetic radiation. The frequency of the radiation is determined by the depth of the cavities and it is hard to tune a magnetron in frequency during operation. It is very stable in frequency though and can generate high powers of several gigawatt. The difference between an ordinary magnetron and an HPM magnetron is the higher voltages and currents, which requires other electrode materials.

The MILO (Magnetically Insulated Line Oscillator) is basically a linear magnetron [6], see Figure 1.3. The big difference compared to an ordinary cylindrical magnetron is that the MILO does not require an external magnetic field. The current itself generates an axial magnetic field that prevents the electrons to short-circuit the anode-cathode gap. To generate the self insulating magnetic field an applied voltage of >500 kV is needed. Since much of the energy goes to the magnetic field the MILO has lower efficiency than the magnetron.

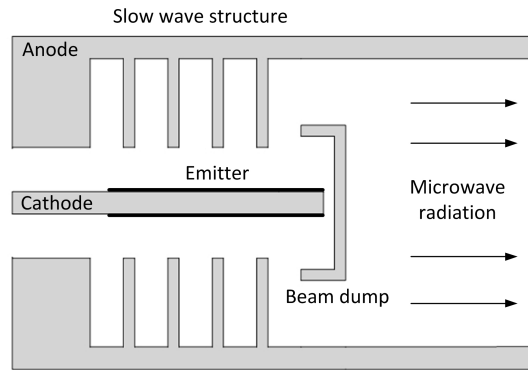


Figure 1.3: MILO. The current generates an axial magnetic field that prevents the electrons from short-circuiting the anode-cathode gap.

In a relatron an electron beam travels through a cavity where the beam bunches. The bunched beam is then accelerated in a gap with a high applied voltage, to a velocity close to the speed of light, see Figure 1.4 [7]. The relativistic speed freezes the bunching and the velocity spread of the electrons is low, with monochromatic radiation as a result. The microwave radiation is extracted in one or several cavities.

This thesis is based on experiments with the vircator and it will be more thoroughly described in following chapters.

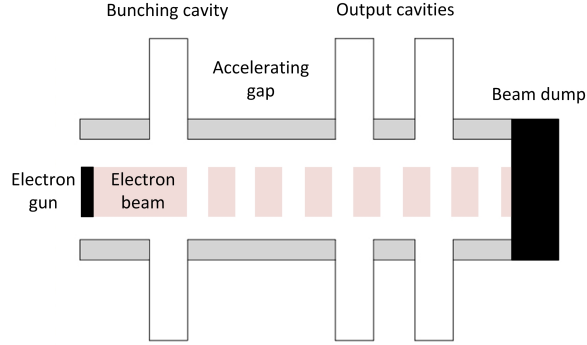


Figure 1.4: Relatron. The electron beam is bunched in the first cavity. The bunched beam is then accelerated to relativistic speed, which freezes the bunching. This leads to less velocity spread of the electrons and the radiation becomes monochromatic.

1.2 Vircators

The vircator (virtual cathode oscillator) differs from the rest of the HPM sources in the way that microwave radiation is not generated from the interaction of an electron beam and a cavity. Electrons are emitted from the cathode and accelerated towards the anode. The anode of the vircator is transparent to electrons and the electron beam passes through the it, see Figure 1.5. The physics behind the vircator operation is that there is a limit to how much current an electron beam can carry. If this limit is reached the potential energy from the space charge in the electron beam is higher than the beam's kinetic energy and an electron cloud, a virtual cathode, is formed. When this electron cloud oscillates and when electrons are reflected between the cathode and the virtual cathode, microwave radiation is generated.

HPM sources like the vircator require high voltages and currents and the performance of the source depends highly on the electrode materials (Paper I and III). Common emitter materials are velvet, carbon fibre or other materials with sharp tips. For dielectric materials like velvet, the electrons are emitted with explosive field emission, where the electrons are emitted from a plasma that is formed around the fibres [8, 9, 10]. To much

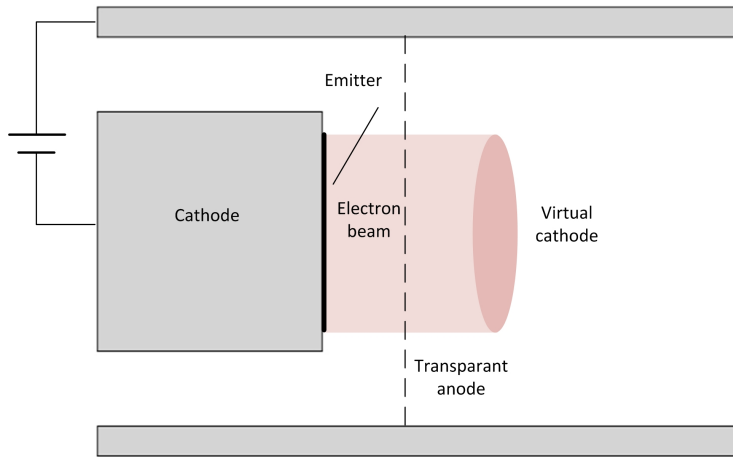


Figure 1.5: Schematic vircator. Electrons are emitted from the cathode and accelerated towards and then through the transparent anode. A virtual cathode is formed when the space charge limit is reached.

plasma lowers the vacuum quality which in turn lowers the performance of the vircator. To reduce plasma formation a conducting emitter material like carbon velvet can be used [11, 12, 13], where the electrons are emitted by field emission [14]. An applied electric field is enhanced at the tips and the electrons are allowed to tunnel directly from the material into vacuum.

A vircator can be designed in different ways. Three most common geometries are the axial [15] and coaxial vircators [16], and the reflex triode [17], see Figure 1.6. In the axial vircator and the reflex triode the anode and cathode are parallel and have the same center axis, while the anode and cathode of the coaxial vircator are cylinders sharing the same center axis. The reflex triode is positively pulsed on the inner conductor while the axial and coaxial vircators usually are negatively pulsed.

To improve the performance of the vircator the virtual cathode can be enclosed in a resonance cavity [18]. If the cavity is tuned to the operating frequency, higher fields can be extracted. Vircators tend to have a frequency chirp during the pulse but a resonance cavity can stabilize the frequency. In the axial vircator and the reflex triode the cavity can be a pillbox attached to the anode, enclosing the virtual cathode. The housing of the axial vircator

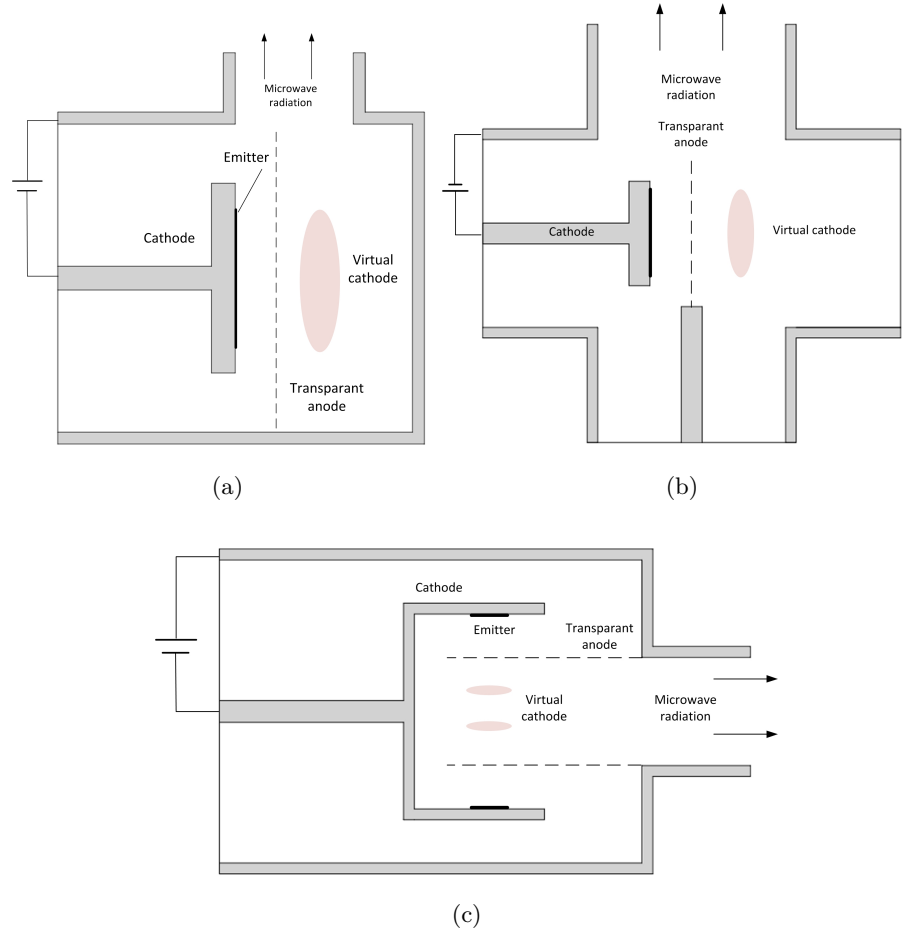


Figure 1.6: Three common vircator types. a) Axial vircator b) Coaxial vircator c) Reflex triode

tor is also a cavity defined by the vacuum tube and the wall to the right in Figure 1.6a). This wall can be moved in the axial direction (see Paper III) to find the optimum position. In the coaxial vircator the cathode and anode act as cavities.

In order to generate high powers a high current is needed and this requires a large emitting area. The coaxial vircator has the emitting area

over the circumference of the cathode and therefore the axial width of the emitter can still be small. With a narrower electron beam there can be a more defined excitation point for the generated microwave radiation.

2. Experiments and theoretical models

Some basic properties of a vircator, like the operating frequency and current, can be estimated quite well with analytical expressions. Better estimates can be made with computer simulations but even though the geometry of the vircator is simple, it is hard to predict the performance. Experiments are therefore very important in the understanding of vircator physics. Generation of HPM differs from other microwave generation in that the pulses are very short and have high peak power. This puts quite different requirements on the HPM equipment. There are hardly any off-the-shelf HPM products and those that can be bought are expensive and not always ideal for the purpose. Therefore much in-house products are used.

2.1 Vircator theory

All particles in the electron beam carry a charge and together they create which will give the electron beam potential energy. At a distance of approximately the anode-cathode gap from the anode, the potential energy of the electron beam is higher than the kinetic energy. A negative potential well is formed and the beam electrons will reflect and the current is stopped. When this happens the space charge limit is reached and an electron cloud, a virtual cathode, is formed.

Figure 2.1 shows a 3D particle in cell (see Chapter 2.3) simulation at a time in the simulation when the vircator operation is stable. The figure shows the relative momentum of the electrons along the center axis of an axial vircator. The electrons are emitted at the cathode and are accelerated towards the anode with a positive velocity. The electrons have the maximum speed at the anode and slow down after they have passed it. After

the virtual cathode is formed it continues to grow and the space charge increases. A higher space charge stops electrons with higher velocities and the virtual cathode moves closer to the anode until it is so close that the kinetic energy of the electrons are high enough to pass the virtual cathode. When this happens the virtual cathode is dissolved and the electron beam can propagate again. This can be seen in the figure as escaping electrons. When the current in the electron beam has reached the space charge limit again, a new virtual cathode is formed. This periodic formation of virtual cathodes creates an oscillation that generates a part of the electromagnetic radiation. The time between the generation of two virtual cathodes agrees well with the period of the generated microwave radiation. The electrons with negative momentum are those that have been reflected back from the virtual cathode. These electrons will also generate radiation when they reflex between the cathode and virtual cathode. The reflexing electrons will not necessary have the same frequency as the oscillation of the virtual cathode. If these two processes are forced to radiate at the same frequency, *e.g.* by using resonance cavities, better performance of the vircator can be achieved.

The space charge limiting current I_{SCL} for a cylindrical electron beam can be expressed as [19]

$$I_{SCL} = 2\pi\epsilon_0 \frac{m_0 c^3}{e} \frac{(\gamma^{2/3} - 1)^{3/2}}{1 + 2 \ln(R/r_b)}, \quad (2.1)$$

where ϵ_0 is the permittivity of free space, m_0 is the rest mass of an electron, c is the speed of light, R is the radius of the vacuum tube and r_b is the electron beam radius. The relativistic factor γ is defined as

$$\gamma = \sqrt{\frac{1}{1 - v^2/c^2}}, \quad (2.2)$$

where v is the speed of the electrons.

The virtual cathode oscillates with approximately the plasma frequency of the electron beam. The plasma frequency f_p for a planar geometry is given by

$$f_p = \frac{1}{2\pi} \sqrt{\frac{n_b e^2}{\epsilon_0 m_0 \gamma}} \quad (2.3)$$

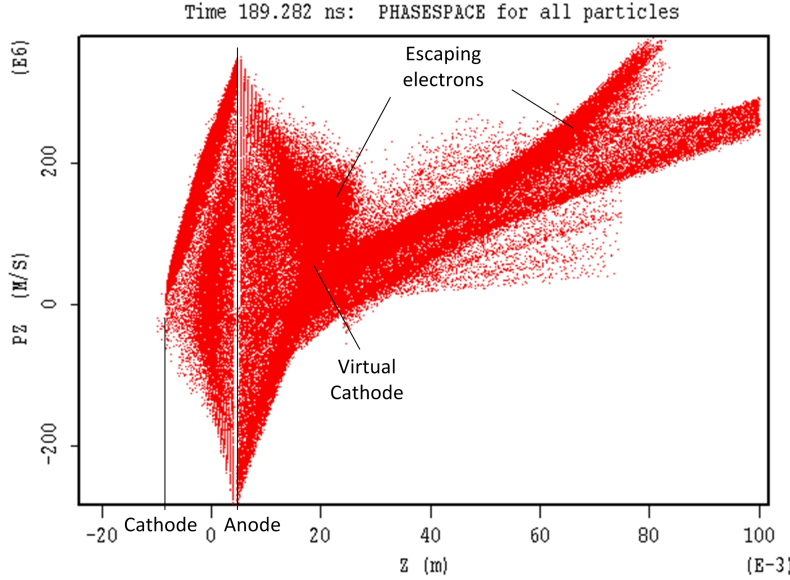


Figure 2.1: Particle in cell simulation of an axial vircator showing the relative momentum of the electrons on the center axis. A virtual cathode is beginning to form at a distance of about the anode-cathode distance. Before a new virtual cathode is formed electrons escape from the virtual cathode area.

where $-e$ is the electron charge and n_b is the electron density in the beam as it passes through the anode. The relativistic factor γ can in a vircator also be derived from the relativistic energy conservation law

$$(\gamma - 1)m_0c^2 = eU, \quad (2.4)$$

where U is the voltage over the anode-cathode gap.

For voltages less than 500 kV, a non relativistic approximation can be made, and the electron density can be derived from the Child-Langmuir relation of a planar diode, which describes the maximum current density j_{CL} that can be obtained.

$$j_{CL} = \frac{4}{9} \sqrt{\frac{2e}{m_0}} \frac{U^{3/2}}{4\pi d^2} = n_b e v, \quad (2.5)$$

where d is the anode-cathode gap distance. The electron velocity v at the anode can now be obtained from the non relativistic energy conservation

relation

$$\frac{m_0 v^2}{2} = eU. \quad (2.6)$$

The radiation generated when electrons are reflected between the virtual cathode and the cathode does not necessary have the same frequency as the virtual cathode oscillation. This frequency for a vircator without resonant cavities or feed back, can be determined from the time it takes for one electron to travel from the cathode to the virtual cathode and back again, a distance that is about four times the anode-cathode gap. The transit time τ_0 between cathode and anode is

$$\tau_0 = \frac{d}{v} \quad (2.7)$$

and the frequency of the reflected electron is

$$f_r = \frac{1}{2\pi \tau_0} = \frac{3}{16} \sqrt{\frac{2eU}{m_0 d^2}}. \quad (2.8)$$

2.2 Experimental setup

All experiments were performed at the HPM laboratory at FOI in Grindsjön. The experimental setup consists of vircator, voltage generator, vacuum pump, shielded operating room, and an anechoic chamber where the microwaves are radiated and the microwave probes are situated, see Figure 2.2 and 2.3. The anechoic chamber has metal walls and the interior dimensions are $2.4 \times 5.9 \times 2.4$ m. On the inside it is covered with 20 cm thick microwave absorbers.

In the experiments an axial vircator was used. It is housed inside a standard three-way ConFlat 8"-6"-8" vacuum tee. The generated microwaves are radiated through a 2 m long waveguide connected to the 6" center port of the tee. The voltage source and vacuum pump are connected to the other two ports. The axial vircator is designed so that the generated microwaves can be extracted either only from the area between the anode and cathode, or from both sides of the anode, see Figure 2.4. In the first case, only the radiation from reflexing electrons in the anode-cathode gap is extracted.

The depth of the resonance cavity can be changed by moving the wall. The cathode and anode are designed so that different electrode materials

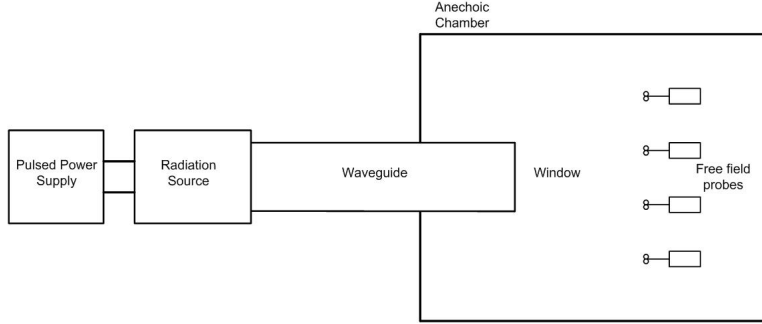


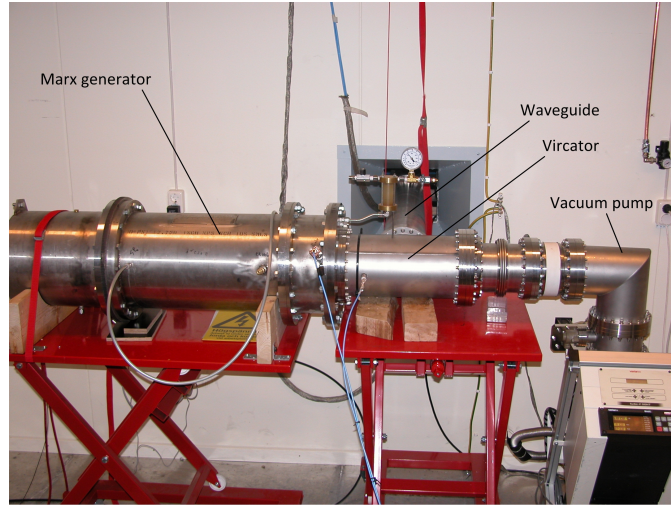
Figure 2.2: Schematic figure of the HPM lab.

can be used, and the distance between them can be changed.

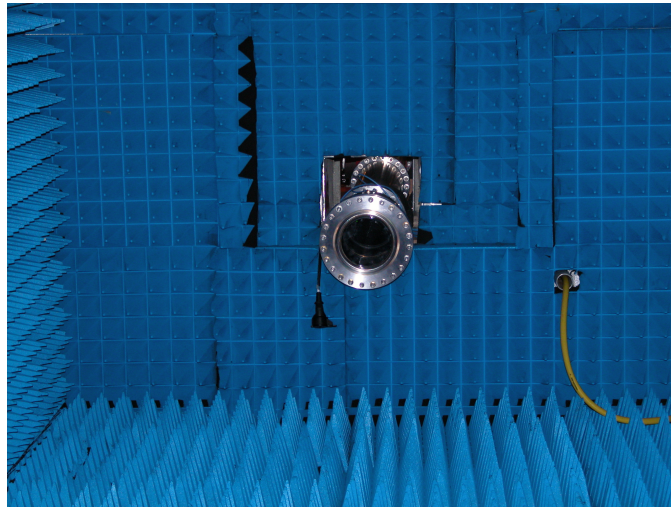
The vircator is powered by a Marx generator [20], a voltage generator where capacitors are charged in parallel and discharged in series via spark gaps, see Figure 2.5. The Marx generator has 25 stages resulting in a nominal output voltage of 400 kV and a nominal energy of 320 J [21]. The Marx generator can be set to deliver up ten pulses in one second.

During the experiments the Marx generator was charged to an erected voltage of 385 kV, resulting in a peak voltage of about 250 kV across the anode-cathode gap. The peak-voltage jitter between shots was about 5%. The stored energy in the Marx generator was 300 J. The voltage was measured with a capacitive divider with a rise time of 30 ns, and the current was measured with a Rogowski coil [22] with a rise time of 20 ns.

To measure HPM pulses special probes are needed since the pulses are short and the electromagnetic field strength high. The probes must have a short rise time to be able to record the rapid changes of the microwave radiation and a small effective area, otherwise there will be a flashover at the output of the probe. One probe that meets these requirements is the B-dot probe, which basically is a small single loop antenna that measures the time derivative of the magnetic field. To lower the inductance and thus giving it a shorter rise time the loop is extended in the axial direction to a cylinder. In order to obtain a differential output two cylinders are used measuring in opposite directions, see Figure 2.6. When the signals from the two cylinders are added together, the signal is doubled and common mode noise is canceled out.



(a)



(b)

Figure 2.3: HPM lab. The microwave radiation is propagated through a 2 m long waveguide. a) Marx generator, vircator and vacuum pump. b) Waveguide aperture in the anechoic chamber.

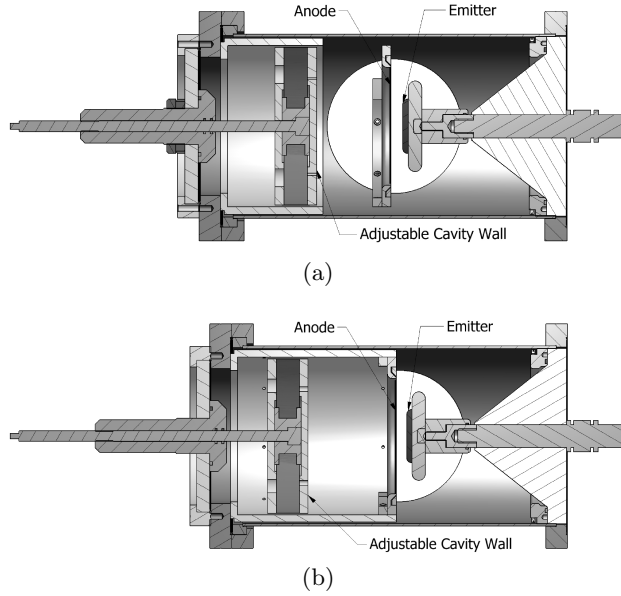
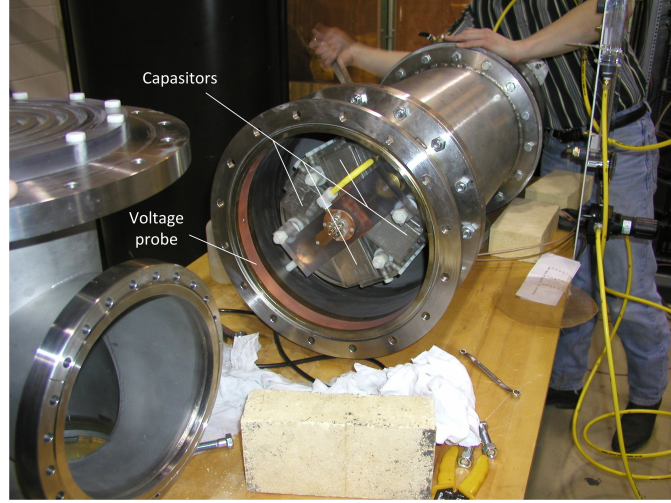


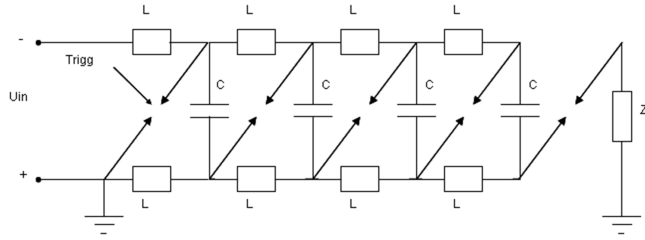
Figure 2.4: Axial vircator with different extraction possibilities. The adjustable cavity wall is used to tune the cavity. a) Extraction from both sides of the anode. b) Extraction only from the anode-cathode side. Radiation generated by the virtual cathode is not extracted.

To be able to determine the radiation pattern measurements at several points have to be made. Since there are shot-to-shot variations, measurements of the radiation pattern have to be made at all desired positions at the same time, which requires many probes. The probes are expensive and measurements of probes have shown that our in-house built probes perform as good as commercial ones. Another advantage with building own probes is that they can be modified to meet new requirements. Both commercial and in-house probes are calibrated at SP Technical Research Institute of Sweden. To verify that the probes perform as intended they are also tested regularly in the lab using standard gain horn antennas and a network analyzer.

It is difficult to build small, wideband antennas with a flat frequency response. It is therefore important to compensate for the frequency dependence and attenuation of the probes and cables in the postprocessing of data (Paper II). This is especially important with a source like the vircator since the operating frequency of the vircator tends to shift during the pulse.



(a)



(b)

Figure 2.5: a) Marx generator with 25 stages. Here only the last stage is visible. The capacitive voltage divider probe can also be seen. b) Circuit drawing with four stages. The capacitors C are charged in parallel and when the first spark gap is triggered, the rest of the spark gaps close. The capacitors are then discharged in series and the voltage over the load Z_L is four times the input voltage.

2.3 Design tools

To be able to simulate both charged particles and time varying electromagnetic fields, a method called particle-in-cell (PIC) can be used [23]. A mathematical grid is put over the simulation volume. In the cells the total

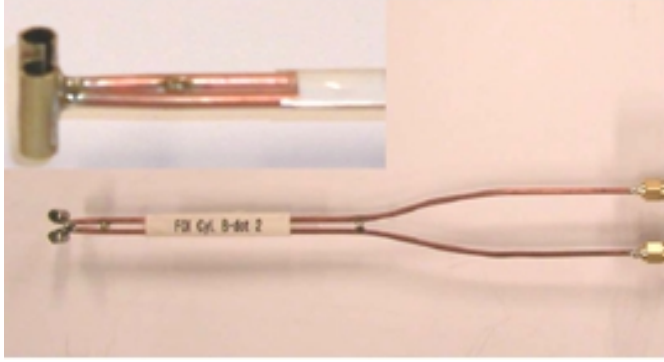


Figure 2.6: B-dot probe.

charge is represented by super-particles each with the total mass and charge as the original particles, thus keeping the original charge to mass ratio, see Figure 2.7. The charge of each super-particle is distributed on the grid points and are weighted with the distance to the grid points. The resolution gets better with the number of super-particles. The use of super-particles reduces simulation time significantly compared to simulating all particles.

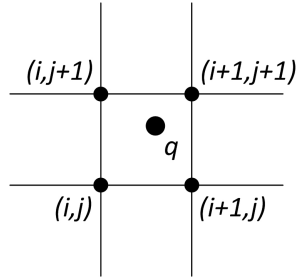


Figure 2.7: 2D PIC grid

The equations to be solved for are the Lorentz' force equation for the movement of the super-particles

$$m \frac{d\mathbf{v}}{dt} = q (\mathbf{E} + \mathbf{v} \times \mathbf{B}), \quad (2.9)$$

and the Maxwell equations

$$\nabla \times \mathbf{E} = -\frac{\partial \mathbf{B}}{\partial t} \quad (2.10)$$

$$\nabla \times \mathbf{B} = \mu_0 \mathbf{J} + \frac{1}{c^2} \frac{\partial \mathbf{E}}{\partial t}. \quad (2.11)$$

m , \mathbf{v} and q are the mass, velocity and charge of the particle. \mathbf{E} and \mathbf{B} are the electric and magnetic fields, μ_0 is the permeability of free space and c is the speed of light. These equations are solved with the following iteration cycle:

1. Assign the charge on the grid points
2. Solve the electric and magnetic fields
3. Calculate the Lorentz' forces on the super-particles
4. Move the super-particles

One way to solve these equations is with a Finite-Difference Time-Dependent (FDTD) method, which is second-order accurate in both time and space. Maxwell's equations can be solved with the Yee algorithm which solves both the electric and magnetic fields in time and space. The Yee algorithm has a staggered grid and uses central difference for the space derivatives and leapfrog for the time derivatives, see Figure 2.8. Leapfrog time-stepping means that the electric and magnetic fields are not calculated at the same time step.

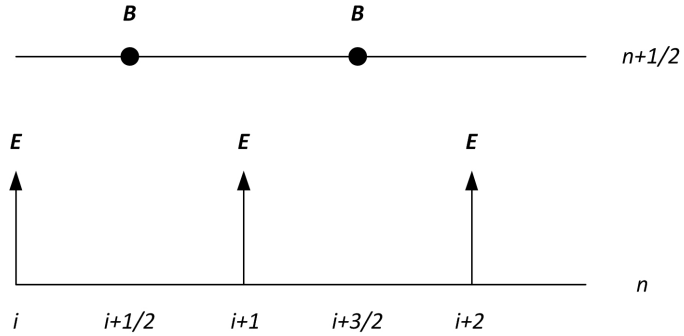


Figure 2.8: 1D Yee scheme. The electric field is calculated at integer time and space steps while the magnetic field is calculated at half integer steps. The index is n for the time stepping and i for the space stepping.

In the one-dimensional case (2.10) becomes

$$\frac{E_{z, i+1}^n - E_{z, i}^n}{\Delta x} = - \frac{B_{y, i+1/2}^{n+1/2} - B_{y, i+1/2}^{n-1/2}}{\Delta t} \quad (2.12)$$

for a wave polarized in the z -direction, where Δx and Δt are the steps in space and time. The electric field and super-particle position are solved at integer time steps and the magnetic field, current density and super-particle velocity are solved at half integer time steps.

3. Results

3.1 Paper I

Experimental studies of anode and cathode materials in a repetitive-driven axial vircator

Repetitive use of a high-power-microwave radiation source implies strong erosion on cathode and anode materials. Electrode-material endurance has been studied in a series of experiments with an axial virtual cathode oscillator powered by a compact Marx generator. The Marx generator is operated in a 10-Hz repetitive mode with a burst of ten pulses. Velvet and graphite was used as emitter material and stainless-steel mesh, stainless-steel wires, and molybdenum wires as anode material. The voltage and current of the vircator was studied with different combinations of electrode materials. The most commonly used electrode materials, velvet emitter and stainless steel mesh anode, showed the largest shot-to-shot variations while the combination graphite emitter and molybdenum wires showed a more repetitive behavior, but with lower radiated field strengths and shorter pulse lengths.

Destructive tests, where the number of shots before failure was registered, showed that the best results from the combination of graphite emitter and molybdenum wire anode.

3.2 Paper II

Magnetic Field Measurement System for HPM Research

One method to characterize the radiated microwave field from a high-power microwave (HPM) source is to measure the radiated high-level electromagnetic field in several locations at a high sampling rate registering the fre-

quency time dependence, thus being able to determine the radiated pattern and mode. A complete free-field measurement system for measuring the magnetic field component in high-level electromagnetic fields has been developed at FOI. The system consists of a B-dot sensor and a balun, both designed and constructed at FOI. The B-dot sensor is designed as two cylindrical loop sensors with differential output. The balun is a microstrip design etched on a dual sided PTFE circuit board.

The B-dot sensor is used to measure very high field strengths, and to avoid electrical breakdown it is important that the gain is low. The B-dot sensor and balun is used in a large frequency band, 1–6 GHz, and it is in practice impossible to get a flat frequency response for such a system. This use of an antenna is quite unconventional, since it is more common to design antennas with high gain and only use them within a frequency band where the frequency response is flat, and where theoretical models agree well.

Due to the large frequency band in which the B-dot sensor is used, resonances in the system can give an output signal from the B-dot sensor and balun that is several times higher at times when the frequency shifts some hundred megahertz, even though the actual magnetic field strength is the same.

Since the B-dot sensor and balun have to be small, they are hard to build and all B-dot-balun pair have slightly different characteristics. To get accurate measurements, all pairs have been individually calibrated at SP Technical Research Institute of Sweden. In the postprocessing, the signal registered at the oscilloscope is compensated for the frequency dependence of the B-dot-balun pair used.

3.3 Paper III

Experimental Studies of the Influence of a Resonance Cavity in an Axial Vircator

A resonance cavity enclosing the virtual cathode can improve the performance of a vircator. Experiments with different cavity depths have been made to test if it is possible to make the two radiating mechanisms of the vircator radiate at the same frequency. In this experiment series it was very important to have low shot-to-shot variations to be able to see the cavity variations, and not the cathode material deterioration. Carbon fibre velvet

was used as emitter material and molybdenum wires as anode. The carbon fibre velvet combines the good qualities of the emitter materials tested in Paper I, the low shot-to-shot variation of graphite and the high radiated fields and longer pulse lengths of velvet.

To be able to study the two radiation mechanisms of the vircator, it was designed so that the radiation from the virtual cathode can be shielded off. Only radiation from the area between the anode and cathode is then extracted. The depth of the resonance cavity showed to have small influence on the radiation from the volume between the anode and cathode. At the optimum cavity depth the virtual cathode was forced to oscillate at the same frequency as the electrons in the anode-cathode gap. The result was a very narrow bandwidth of the microwave radiation, less than one percent, which is unusual for an axial vircator. At this cavity depth the magnetic field strength was the highest registered. The use of a cavity also made the microwave pulse stable in frequency during the entire pulse.

4. Discussion

Generation of High Power Microwaves is a research area facing many problems not common in generation of microwaves with lower power. The materials have to withstand very high currents and voltages, and special care has to be taken in the material choices. The performance of a vircator can, like most microwave sources, be optimized. To be able to do reliable geometrical studies the shot-to-shot variations have to be low. Experiments have shown that even different velvet fabrics result in different characteristics of the microwave radiation, voltage and current. We have tested many electrode materials and found that carbon fibre velvet is the best emitter material. Unfortunately we have only one carbon fibre emitter and we have not been able to get hold of more of that kind. The search for new emitter materials is therefore an ongoing process, and the goal is to find a material with a low emission threshold, low outgassing and that can be manufactured in different geometries.

Narrow band HPM research has mostly sprung out of pulsed power and plasma physics and, traditionally, low effort has been put on the measurement system. In the postprocessing of vircator experiment data it obvious that compensating for the entire frequency response of the measurement system is necessary. For a radiation source like the vircator, where the frequency may shift during the pulse, it is extremely important to compensate for the entire frequency response while it may be enough to just use the dominating frequency in the postprocessing for a more frequency stable source, like the magnetron.

5. Conclusions

The vircator is a narrow band HPM source with a simple geometry. It is possible to build compact vircators since they do not require an external magnetic field and can be driven by non relativistic voltages. The performance of the vircator depends highly on the electrode materials. Carbon fibre velvet has been shown to have low shot-to-shot variations and the generated field strengths of the microwave radiation are high compared to *e.g.* graphite. If the vircator is to be used repetitively the erosion of the electrode materials must be low. Molybdenum wires as anode material have proven to last much longer than stain-less steel wires.

To be able to properly evaluate the performance of the radiation source, a well known measurement system must be used. Special far-field probes are required to measure the high generated fields of an HPM source. To avoid electrical breakdown the probes must have a low gain, which in our case is achieved with small aperture areas of the probes. The diameter of the probe is just a few percent of the wavelength of the microwaves. The probes are used in a wide frequency range, 1–6 GHz, in which the frequency response is not flat. The actual frequency response may differ several decibel from the theoretical due to resonances in the measurement system. For conventional antenna use the variations are too large, but for HPM use it is fully sufficient as long as the measurements are compensated for the frequency response of the measurement system. Since the frequency of the pulses may shift during the pulse and also differ between shots with identical setup due to *e. g.* jittering in the voltage supply it is important to compensate for the entire frequency response and not only the dominating frequency. We have developed our own measurement system and each individual probe is calibrated.

With proper electrode materials and a well calibrated measurement system it is possible to make geometry optimization studies. We have shown

with experiments that it is possible to make the two radiation mechanisms of the vircator radiate at the same frequency. By including a tuned resonance cavity in the vircator geometry the virtual cathode can be forced to oscillate with the same frequency as the radiation from the electrons that are reflected between the cathode and virtual cathode. The result is higher radiated microwave fields with a very narrow bandwidth.

References

- [1] M. Abrams, “The dawn of the e-bomb”, *IEEE Spectrum*, volume 40, pp. 24–30, 2003.
- [2] J. Benford, J. Swegle and E. Schamiloglu, *High Power Microwaves Second Edition*, Taylor & Francis, 2007.
- [3] R. Barker and E. S. (Eds.), *High-Power Microwave Sources and Technologies*, IEEE Press, 2001.
- [4] R. Hoad, N. Carter, D. Herke and S. Watkins, “Trends in em susceptibility of it equipment”, *IEEE Trans. Electromag. Compability*, volume 46, pp. 390–395, 2004.
- [5] S. Gold and G. Nusinovich, “Review of high-power microwave source research”, *Rev. Sci. Instrum.*, volume 68, pp. 3945–3974, 1997.
- [6] M. Clark, B. Marder and L. Bacon, “Magnetically insulated transmission line oscillator”, *Appl. Phys. Lett.*, volume 52, pp. 78–80, 1988.
- [7] R. Miller, W. McCullough, K. Lancaster and C. Muehlenweg, “Super-relatron theory and experiments”, *IEEE Trans. Plasma Sci.*, volume 20, pp. 332–343, 1992.
- [8] D. Shiffler, M. Ruebush, M. LaCour, K. Golby, R. Umstattd, M. C. Clark, J. Luginsland, D. Zagar and M. Sena, “Emission uniformity and emission area of explosive field emission cathodes”, *Appl. Phys. Lett.*, volume 79, pp. 2871–2873, 2001.
- [9] R. J. Adler, G. F. Kiuttu, B. E. Simpkins, D. J. Sullivan and D. E. Voss, “Improved electron emission by use of a cloth fiber cathode”, *Rev. Sci. Instrum.*, volume 56, pp. 766–767, 1985.

- [10] R. B. Miller, “Mechanism of explosive electron emission for dielectric fiber (velvet) cathodes”, *J. Appl. Phys.*, volume 84, pp. 3880–3889, 1998.
- [11] D. Shiffler, M. Ruebush, M. Haworth, R. Umstattd, M. LaCour, K. Golby, D. Zagar and T. Knowles, “Carbon velvet field-emission cathode”, *Rev. Sci. Instrum.*, volume 73, pp. 4358–4362, 2002.
- [12] E. Garate, R. D. McWilliams, D. E. Voss, A. L. Lovesee, K. J. Hendricks, T. A. Spencer, M. C. Clark and A. Fisher, “Novel cathode for field-emission applications”, *Rev. Sci. Instrum.*, volume 66, pp. 2528–2532, 1995.
- [13] A. Roy, R. Menon, S. Mitra, S. Kumar, V. Sharma, K. Nagesh, K. Mittal and D. Chakravarthy, “Plasma expansion and fast gap closure in a highpower electron-beam diode”, *Phys. Plasmas*, volume 16, p. 053103, 2009.
- [14] R. H. Fowler and L. Nordheim, “Electron emission in intense electric fields”, *Proc. R. Soc. A*, volume 119, pp. 173–181, 1928.
- [15] S. Burkhart, “Multigigawatt microwave generation by use of a virtual cathode oscillator driven by a 1–2 MV electron beam”, *J. Appl. Phys.*, volume 62, pp. 75–78, 1987.
- [16] W. Jiang, K. Woolverton, J. Dickens and M. Kristiansen, “High power microwave generation by a coaxial virtual cathode oscillator”, *IEEE Trans. Plasma Sci.*, volume 27, pp. 1538–1542, 1999.
- [17] R. A. Mahaffey, P. Sprangle, J. Golden and C. A. Kapetanakis, “High-power microwaves from a nonisochronic reflecting electron system”, *Phys. Rev. Lett.*, volume 39, pp. 843–846, 1977.
- [18] J. Benford, D. Price, H. Sze and D. Bromley, “Interaction of a vircator microwave generator with an enclosing resonant cavity”, *J. Appl. Phys.*, volume 61, pp. 2098–2100, 1987.
- [19] R. Miller, *An Introduction to the Physics of Intense Charged Particle Beams*, Plenum Press, 1982.
- [20] P. Smith, *Transient Electronics Pulsed Circuit Technology*, John Wiley & Sons, 2002.

- [21] A. Neuber, Y. Chen, J. Dickens and M. Kristiansen, “A compact, repetitive, 500 kv, 500 j, marx generator”, in “Proc. 15th IEEE Int. Pulsed Power Conf., Monterey, CA”, pp. 1203–1206, June 2005.
- [22] D. G. Pellinen, M. S. D. Capua, S. E. Sampayan, H. Gerbracht and M. Wang, “Rogowski coil for measuring fast, high-level pulsed currents”, *Rev. Sci. Instrum.*, volume 51, pp. 1535–1540, 1980.
- [23] C. Birdsall and A. Langdon, *Plasma Physics via Computer Simulation*, Taylor & Francis, 2005.